The Effect of Bone-Marrow-Derived Stem Cells and Adipose-Derived Stem Cells on Wound Contraction and Epithelization

Cagri A. Uysal,[1,*] Morikuni Tobita,[2] Hiko Hyakusoku,[3] and Hiroshi Mizuno[2]

[1]Department of Plastic and Reconstructive Surgery, Faculty of Medicine, Baskent University, Ankara, Turkey.
[2]Department of Plastic and Reconstructive Surgery, Juntendo University, Tokyo, Japan.
[3]Department of Plastic and Reconstructive Surgery, Nippon Medical School, Tokyo, Japan.

Cagri A. Uysal, MD, PhD

Submitted for publication March 20, 2014. Accepted March 26, 2014.

*Correspondence: Department of Plastic and Reconstructive Surgery, Baskent University Faculty of Medicine, Fevzi Cakmak Cad. 5. Sok. No: 48, Bahcelievler, Ankara 06490, Turkey (e-mail: cagriuysal@hotmail.com; cagriuysal@yahoo.com).

Objective: The relationship between the wound contraction and levels of α-smooth muscle actin (α-SMA) has been revealed in different studies. We aimed to investigate the effects of mesenchymal stem cells (MSCs), mainly bone-marrow-derived stem cells (BSCs) and adipose-derived stem cells (ASCs), and find out the α-SMA, fibroblast growth factor (FGF), transforming growth factor beta, and vascular endothelial growth factor (VEGF) levels on an *in vivo* acute wound healing model after the application of MSCs.

Approach: Four circular skin defects were formed on the dorsum of Fisher rats ($n=20$). The defects were applied phosphate-buffered saline (PBS), ASCs, BSCs, and patchy skin graft, respectively. The healing time and scar area were noted.

Results: There was a statistical decrease in the healing time in ASC, BSC, and skin graft groups ($p<0.05$). However, the scar was smaller in the PBS group ($p<0.05$). The α-SMA levels were statistically lower in ASC, BSC, and graft groups ($p<0.05$). The FGF levels were statistically higher in ASC and BSC groups ($p<0.05$). The differentiation of the injected MSCs to endothelial cells and keratinocytes was observed.

Innovation and Conclusion: MSCs decrease the healing time and contraction of the wound while increasing the epithelization rate by increasing angiogenesis.

INTRODUCTION

Wound healing is the natural process of regenerating dermal and epidermal tissues. A set of complex biochemical events take place in a closely orchestrated cascade to repair the damage. These events have been artificially categorized into four steps: hemostasis, inflammation, proliferation, and remodeling. The stem cells of the tissue localized to the region or from the blood circulation supply the necessary cell source and thus control this cascade. In its natural course, named as secondary healing, the wound is repaired as soon as possible by granulation, epithelization, and by contraction.[1,2] The key elements are keratinocytes; the fibroblasts rich in actin, called myofibroblasts; and transforming growth factor beta (TGF-β).[3,4]

Differentiation of fibroblasts into myofibroblasts is closely associated with the expression of α-smooth muscle actin (α-SMA).[5–7] Myofibroblasts are the main contractile element during the wound healing and it was shown that the levels of α-SMA expression were correlated with the contractile activity of the fibroblasts *in vitro* and *in vivo*.[8–10] Fibroblast growth factor (FGF) is described to downregulate α-SMA by increasing

DOI: 10.1089/wound.2014.0539

the apoptosis of the myofibroblasts.[11] On the other hand, TGF-β is known to promote the differentiation of fibroblasts into myofibroblasts through upregulation of α-SMA expression.[12]

Regenerative medicine has established a new promising experimental and clinical epoch.[13] The angiogenic potential of postnatal somatic stem cells has been reported especially with bone-marrow-derived stem cells (BSCs) and adipose-derived stem cells (ASCs).[14,15] Not only the angiogenic potential by differentiation into endothelial cells but also the control on the secretion of the cytoprotective cytokines and growth hormones could harmonize the wound healing process.[16]

Clinical Problem Addressed: The relationship between the growth hormones and the wound contraction and levels of α-SMA has been revealed in different studies[17,18]; however, the effect of mesenchymal stem cells (MSCs), mainly BSCs and ASCs, on acute wound healing was not investigated. Thus, we aimed to find out the α-SMA, FGF, TGF-β, and vascular endothelial growth factor (VEGF) levels on an *in vivo* acute wound healing model after the application of MSCs.

MATERIALS AND METHODS

Isolation and preparation of stem cells

Bone-marrow-derived stem cells. Ten-week-old male inbred Fisher (F344) rats (Saitama Experimental Animals Supply Corporation Ltd.) were anesthetized with sodium pentobarbital (Nembutal; Dainippon Sumi Tomo Pharma Co. Ltd.) at 35 mg/100 g and the areas of interest were shaved. The bilateral femur and tibia were dissected and then excised. The proximal and distal ends of the bones were removed to access the bone marrow. The bone marrow was placed in a 50-mL centrifuge tube, followed by washing with phosphate-buffered saline (PBS; Gibco-BRL). The cell suspension was centrifuged at 1,300 rpm for 5 min and the pellet was resuspended in control medium (Dulbecco's modified Eagle's medium [DMEM]; Gibco-BRL) containing 10% fetal bovine serum (FBS; Gibco-BRL) and 1% antibiotic–antimycotic (Gibco-BRL). Cells were plated in 100-mm^2 tissue culture plates (Becton–Dickinson) and maintained in control medium at 37°C in 5% carbon dioxide. The medium was replaced every 3 days and the nonadherent cells were discarded. The cultures were monitored with a microscope to assess expansion and cell morphology. To prevent differentiation, cells were harvested at 80–90% confluence with 0.25% trypsin/ethylene diamine tetraaceticacid (EDTA; Gibco-BRL) and neutralized with culture medium. The resulting cell population was passaged and split three ways at each passage. For subsequent *in vivo* studies, we used cultured BSCs of passage 3, isolated from a single rat. Finally, cells were suspended in PBS at a concentration of 1×10^7 cells/1 cm^3 for injection into each experimental group.

Adipose-derived stem cells. Ten-week-old male inbred Fisher (F344) rats (Saitama Experimental Animals Supply Corporation Ltd.) were anesthetized with sodium pentobarbital (Nembutal; Dainippon Sumi Tomo Pharma Co. Ltd.) at 35 mg/kg and shaved. ASCs were harvested and processed according to our established protocol, as described previously.[19,20] The inguinal fat pads were excised and extensively washed with PBS (Gibco-BRL). They were thenfinely minced and incubated for 1 h on 100-mm^2 tissue culture plates (Becton-Dickinson) containing antibiotic medium—DMEM (Gibco-BRL) with 10% FBS (Gibco-BRL), and 1% antibiotic–antimycotic (Gibco-BRL). The tissue was then rinsed three times in PBS for 5 min followed by digestion with 0.15% collagenase (Wako) and vigorous shaking for 30 min at 37°C in a 50-mL centrifuge tube. Next, an equal volume of control medium was added to neutralize the collagenase. Then, the cell suspension was centrifuged at 1,300 rpm (260 *g*) for 5 min and the cell pellet was resuspended with a control medium. After cell counting using trypan blue, the cells were plated at 100-mm^2 tissue culture plates and maintained in the control medium at 37°C in 5% carbon dioxide. The medium was replaced every 3 days and the nonadherent cells were discarded. To prevent differentiation, the cells were harvested at 80–90% confluence and the cultured cells were detached from the culture dishes with 0.25% trypsin/ethylene diamine tetraaceticacid (EDTA; Gibco-BRL), neutralized with culture medium, collected by centrifugation at 1,300 rpm for 5 min at room temperature, and then passaged into 1:3. Only cultured ASCs of passage 3 isolated from one mouse were used in the subsequent *in vivo* studies. The cells were suspended in medium at a concentration of 1×10^7 cells/ mL for injection into each experimental group.

1, 1′-Dioctadecyl-3, 3, 3′, 3′-tetramethylindo carbocyanine labeling of adipose-derived stem cells

1, 1′-Dioctadecyl–3, 3, 3′, 3′-tetramethylindocarbocyanine (DiI) was dissolved in 99% ethanol at a concentration of 25% and stored at −20°C for use. Cells were labeled with fluorescent DiI (Molecular Probes) according to the manufacturer's recommendations; cells in suspension were incubated

with DiI at a concentration of 2.5 μg/mL in PBS for 5 min at 4°C.

Experimental model

All animal procedures were performed in accordance with the guidelines of the Nippon Medical School Animal Care and Use Committee (Approval No. 18-030). On the dorsum of the rats ($n = 20$) four identical skin defects with 20-mm diameter, until the underlying muscle fascia, were done. One milliliter of injection using 1 mL syringe with 26G needle (Terumo) was done to the defect (0.5 mL) and the surrounding wound edges (0.5 mL) depending on the group. Group I: 1 mL PBS; Group II: 1 mL PBS mixed with 1×10^7 ASCs; Group III: 1 mL PBS mixed with 1×10^7 BSCs; Group IV: patchy full-thickness skin grafts harvested from the excised skin during defect formation. The wounds were closed with dressings.

Macroscopical assessment

The wounds were photographed daily and the day of total epithelization was noted. The healed wound without any hair was accepted as the final scar. The area of the scar was calculated using the software Adobe Photoshop7.0®.

Neovascularization assessment by capillary density

Tissue sections at the median line of the harvested scar tissue were done. The tissues were embedded in paraffin for conventional hematoxylin and eosin (HE) stain. Neovascularization was assessed by measuring the number of capillaries in 20 different fields on HE-stained slides (40× magnification).

Epithelial thickness

Tissue sections were taken at the median line of the harvested scar tissue. The tissues were embedded in paraffin for conventional HE stain. Photographs were taken and scaled. Epithelial thickness was evaluated by measuring the length of the epithelial layer from the stratum basale to the stratum corneum in 20 different fields on HE slides (40× magnification). Three length measurements were noted in every field and, to standardize, the measurements were done in every 0.1 mm from the left border to the right border of the photograph of the field.

Evaluation of the DiI-stained ASCs

The consecutive specimens (4 μm) were done from the tissue samples that were taken from the median line of the harvested scar tissue and the anti–von Williebrand Factor (vWF) antibody (Factor VIII [H-19]: sc-27647; Santa Cruz) was done for the confirmation of the vessels. The tissue specimens were incubated with the monoclonal antibody specific for vWF (1:100 dilution) for 1 h at room temperature. Then, they were washed with PBS and incubated with the secondary antibody fluorescein-isothiocyanate (FITC; 1:100 dilution) (fluorescein anti-goat IgG; FI-5000) with a maximum excitation at 490–500 nm for 30 min at room temperature. Then, they were washed with PBS again. The photographs were taken and evaluated with software (LuminaVison; V220 Olympus).

DiI was visible at the 565-nm wavelength. The DiI-positive cells and the hematoxylin staining were also photographed and merged. The photographs were taken and evaluated with software (LuminaVison; V220 Olympus).

Cytokeratin immunohistochemical staining

Consecutive specimens (4 μm) were done from the tissue samples that were taken from the median line of the harvested scar tissue and the anti–pan cytokeratin antibody (mouse monoclonal to pan cytokeratin [ab11214]; Abcam) immunohistochemical staining was performed. The sections were incubated with anti–pan cytokeratin antibody (1:100 dilution) at room temperature for 24 h (overnight incubation) and then washed with PBS. The antibody possessed FITC with a maximum excitation at 490–500 nm so no secondary antibody was necessary. The photographs were taken and evaluated with software (LuminaVison; V220 Olympus).

α-SMA immunohistochemical staining

Consecutive specimens (4 μm) were done from the tissue samples that were taken from the median line of the harvested scar tissue and the anti–α-SMA antibody (rabbit monoclonal to α-SMA [ab32575]; Abcam) immunohistochemical staining was performed. The sections were incubated with anti–α-SMA antibody (1:200 dilution) at room temperature for 1 h and then washed with PBS. The specimens were incubated with the secondary antibody FITC (1:100 dilution) (fluorescein anti-rabbit IgG, FI-5000; Vector) with a maximum excitation at 490–500 nm for 30 min at room temperature and then washed with PBS. The photographs of the specimens under 40× magnifications were taken in 20 different fields at 470–490 nm wavelength under fluorescent filter. All the photographs were taken in same scale. The green color ratio in groups was evaluated using histogram tool (mean intensity value for green in pixels) of the software Adobe Photoshop7.0®.

FGF immunohistochemical staining

Consecutive specimens (4 μm) were done from the tissue samples that were taken from the median

line of the harvested scar tissue and the anti-FGF antibody (sc-1365; Santa Cruz) immunohistochemical staining was performed. The sections were incubated with anti-FGF antibody (1:200 dilution) at room temperature for 1 h and then washed with PBS. The specimens were incubated with FITC at room temperature for 30 min and then washed with PBS. The photographs of the specimens under 40 × magnification were taken in 20 different fields at 470–490-nm wavelength under fluorescent filter. All the photographs were taken in same scale. The green color ratio in groups was evaluated using histogram tool (mean intensity value for green in pixels) of the software Adobe Photoshop7.0®.

TGF-β1, -β2, and -β3 immunohistochemical staining

Consecutive specimens (4 μm) were done from the tissue samples that were taken from the median line of the harvested scar tissue. The anti–TGF-β1, -β2, and -β3 antibody (TGF-β1 [sc-146], TGF-β2 [sc-90], and TGF-β3 [sc-82]; Santa Cruz) immunohistochemical stainings were performed. The sections were incubated with anti–TGF-β1, -β2, and -β3 antibodies separately (1:200 dilution) at room temperature for 1 h and then washed with PBS. The specimens were incubated with FITC at room temperature for 30 min and then washed with PBS. The photographs of the specimens under 40 × magnification were taken in 20 different fields at 470–490-nm wavelength under fluorescent filter. All the photographs were taken in same scale. The green color ratio in groups was evaluated using histogram tool (mean intensity value for green in pixels) of the software Adobe Photoshop7.0®.

VEGF immunohistochemical staining

Consecutive specimens (4 μm) were done from the tissue samples that were taken from the median line of the harvested scar tissue and the anti-VEGF antibody (mouse monoclonal to VEGF [ab28775]; Abcam) immunohistochemical staining was performed. The sections were incubated with anti-VEGF antibody (1:200 dilution) at room temperature for 1 h and then washed with PBS. The specimens were incubated with FITC at room temperature for 30 min and then washed with PBS. The photographs of the specimens under 40 × magnification were taken in 20 different fields at 470–490-nm wavelength under fluorescent filter. All the photographs were taken in same scale. The green color ratio in groups was evaluated using histogram tool (mean intensity value for green in pixels) of the software Adobe Photoshop7.0®.

Statistical analysis

One-way analysis of variance was used to compare the means in each group. The Tukey test for multiple comparisons was performed for the comparison of the epithelization time; scar area; vascular density; and α-SMA, FGF, TGF-β1, TGF-β2, TGF-β3, and VEGF levels between the groups. Tukey test for multiple comparisons was used to analyze the differences in between TGF-β subfamily groups among the groups separately. Differences were regarded as statistically significant for two-tail values of $p < 0.05$ and the data were presented as mean ± standard deviation (SD). The software Analyse-it for Microsoft Excel (version 2.12) was used in every evaluation (Analyse-it Software, Ltd.).

RESULTS

Macroscopical assessment

The mean time for the total epithelization was 54.25 ± 4.89 days in group I, 39.13 ± 3.67 days in group II, 41.52 ± 4.01 days in group III, and 33.25 ± 3.87 days in group IV. There was a statistical difference between group I and groups II, III, and IV ($p < 0.05$). There was no statistical difference between groups II, III, and IV ($p > 0.5$).

The mean area of the scar tissue was 117.33 ± 21.26 mm^2 in group I, 207.45 ± 24.63 mm^2 in group II, 212.67 ± 25.19 mm^2 in group III, and 253.13 ± 30.56 mm^2 in group IV. There was a statistical difference between group I and groups II, III, and IV ($p < 0.05$). There was no statistical difference between groups II, III, and IV ($p > 0.5$; Fig. 1).

Vascular density

The vascular density was 3.12 ± 0.14 in group I, 7.39 ± 0.36 in group II, 6.95 ± 1.13 in group III, and 4.33 ± 1.07 in group IV. There was a statistical significance between group I and groups II and III ($p < 0.05$). There was no statistical difference between group I and group IV ($p > 0.5$).

Epithelial thickness

The epithelial thickness was found out to be 0.012 ± 0.009 mm in group I, 0.024 ± 0.007 mm in group II, 0.029 ± 0.015 mm in group III, and 0.032 ± 0.017 in group IV. There was a statistical difference between group I and groups II, III, and IV ($p < 0.05$; Fig. 2).

DiI-positive cells, vWF, and cytokeratin immunohistochemical staining

DiI-positive cells were visible in the photographs that were taken with the fluorescent filter at 545–580 nm at the endothelial lining, which was confirmed with anti-vWF antibody. There were DiI

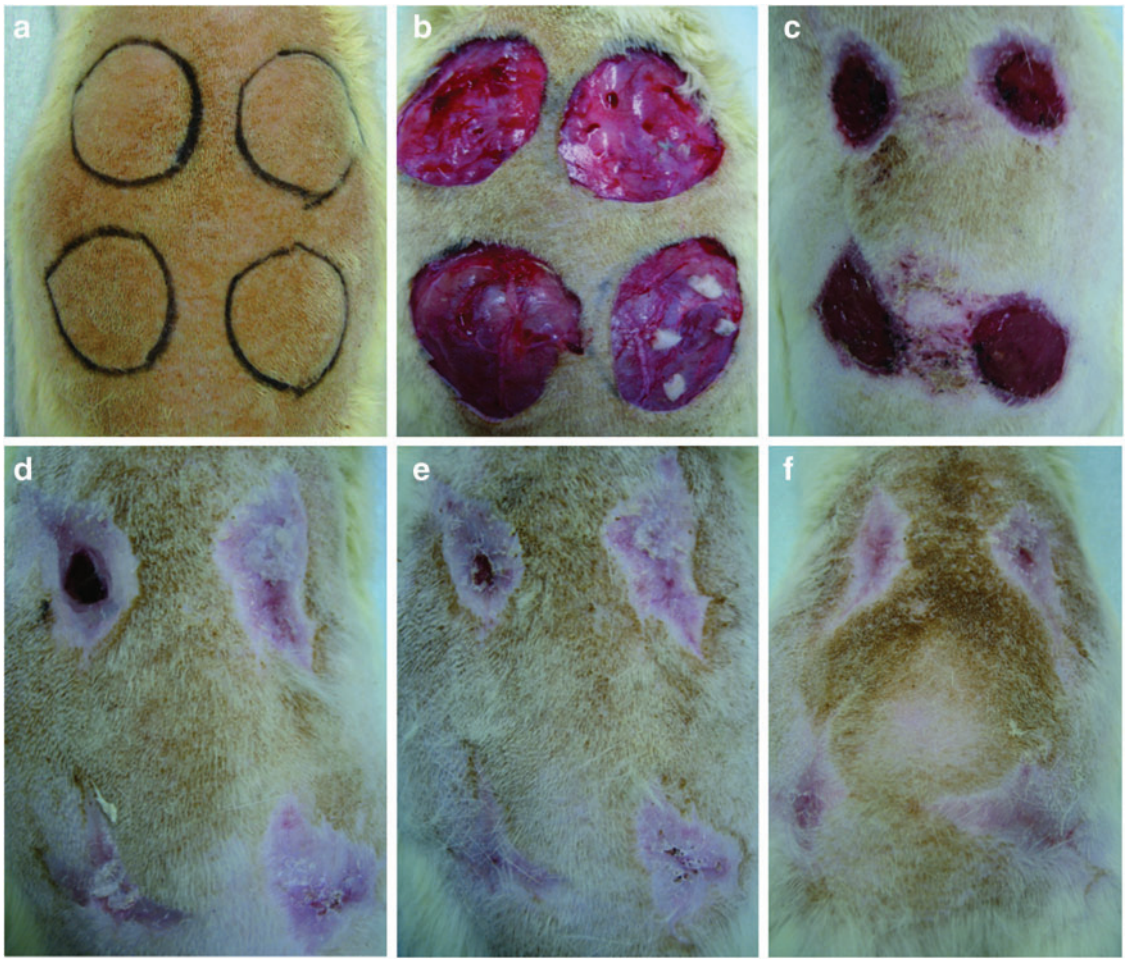

Figure 1. **(a)** Four circular skin defects with a diameter of 20 mm were planned on the dorsum of the rat. **(b)** Group I (left cranial): 1 mL phosphate-buffered saline (PBS) injection; Group II (right cranial): 1 mL PBS mixed with 1×10^7 ASCs; Group III (left caudal): 1 mL PBS mixed with 1×10^7 BSCs; Group IV (right caudal): patchy skin grafts following 1 mL PBS injection. Wound healing progress was photographed on postoperative days 21 **(c)**, 42 **(d)**, 49 **(e)**, and 56 **(f)**. To see this illustration in color, the reader is referred to the web version of this article at www.liebertpub.com/wound

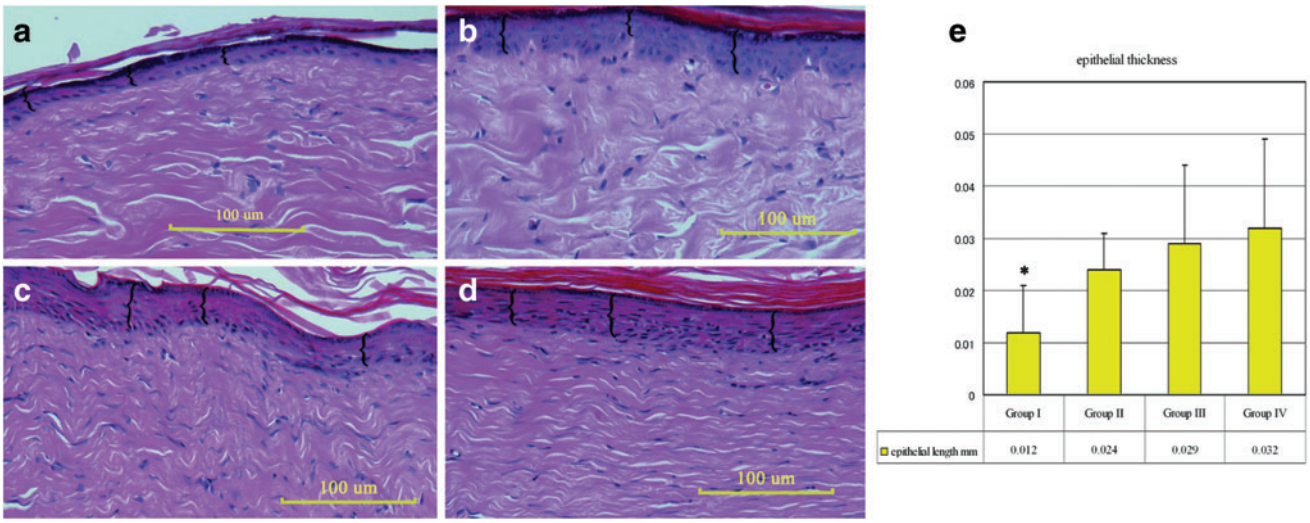

Figure 2. Photographs indicate the hematoxylin and eosin staining of the specimens: groups I **(a)**, II **(b)**, III **(c)**, and IV **(d)**. Braces "{" indicate the length between the stratum basale and stratum corneum calculated in 20 different fields under $\times40$ magnification (scale bar = 100 μm). **(e)** Graph describing the mean epithelial thickness. There was a statistical difference between group I and groups II, III, and IV ($*p<0.05$). To see this illustration in color, the reader is referred to the web version of this article at www.liebertpub.com/wound

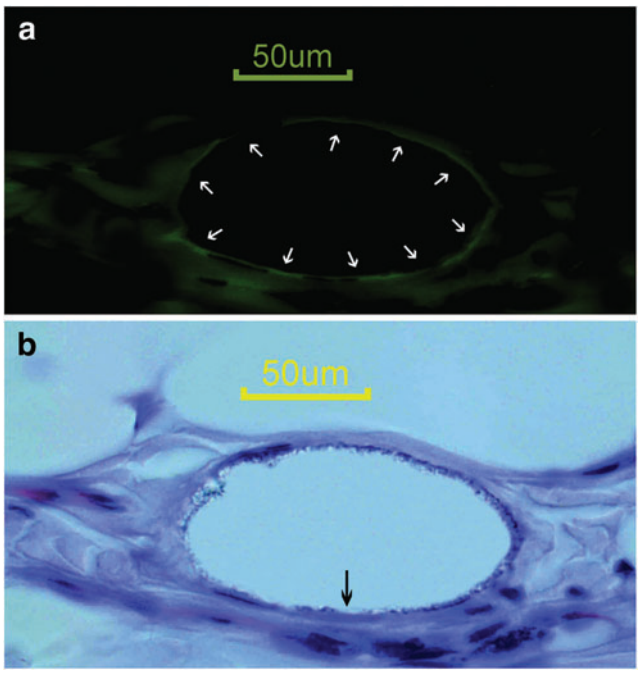

Figure 3. **(a)** Anti-vWF antibody immunohistochemical staining reveals the endothelial lining (white arrows). **(b)** The hematoxylin staining and DiI fluorescence photographs were merged to localize the DiI positivity. The black arrow indicates a DiI-positive endothelial cell (scale bar = 50 μm). To see this illustration in color, the reader is referred to the web version of this article at www.liebertpub.com/wound

and anti-cytokeratin antibody double-positive cells, indicating the *in vivo* differentiation of the BSCs and ASCs to keratinocytes (Figs. 3, 4).

Immunohistochemical evaluation

The mean intensities of the green color for anti–α-SMA antibody immunohistochemical staining were calculated as 45.12 ± 3.68, 18.59 ± 2.84, 19.27 ± 2.17, and 16.33 ± 3.17 in groups I, II, III, and IV, respectively. There were statistically significant decreases in groups II, III, and IV ($p < 0.05$). The mean intensities of the green color for anti-FGF antibody immunohistochemical staining were calculated as 14.81 ± 1.74, 38.51 ± 2.82, 35.28 ± 3.13, and 18.71 ± 3.41 in groups I, II, III, and IV, respectively. There were statistically significant increases in groups II, III, and IV ($p < 0.05$). The mean values for anti–TGF-β1 antibody immunohistochemical staining were calculated as 38.84 ± 1.97, 22.37 ± 2.72, 27.18 ± 3.94, and 34.41 ± 4.77 in groups I, II, III, and IV, respectively. There were statistically significant decreases in groups II and III ($p < 0.05$). The mean values for anti–TGF-β2 antibody immunohistochemical staining were calculated as 36.71 ± 3.58, 19.49 ± 1.56, 22.45 ± 2.62, and 34.83 ± 3.57 in groups I, II, III, and IV, respectively. There were statistically significant decreases in groups II and III ($p < 0.05$). The mean values for anti–TGF-β3 antibody immunohistochemical staining were calculated as 39.52 ± 4.73, 24.72 ± 2.98, 23.15 ± 2.97, and 34.37 ± 4.23 in groups I, II, III, and IV, respectively. There were statistically significant decreases in groups II and III ($p < 0.05$). The mean values for anti-VEGF antibody immunohistochemical staining were calculated as 11.81 ± 1.27, 29.73 ± 3.84, 27.13 ± 2.43, and 13.53 ± 2.07 in groups I, II, III, and IV, respectively. There were statistically significant increases in groups II and III ($p < 0.05$; Fig. 5).

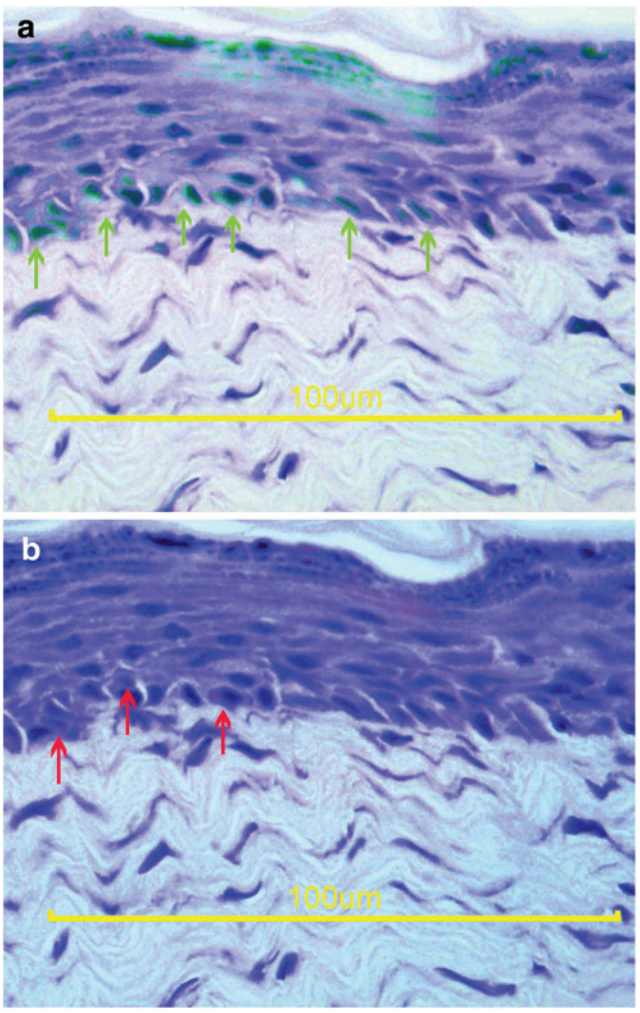

Figure 4. **(a)** The hematoxylin and anti-cytokeratin antibody immunohistochemical stainings were merged to localize the positivity. The green arrows indicate the keratinocytes at the basal membrane. **(b)** The hematoxylin staining and DiI fluorescence photographs were merged to localize the DiI positivity. The red arrows indicate keratinocytes originating from the injected stem cell (scale bar = 100 μm). To see this illustration in color, the reader is referred to the web version of this article at www.liebertpub.com/wound

DISCUSSION

In the natural course of the acute wound healing, the three main processes are epithelization, granulation, and contraction. The MSCs of the environment and from the blood circulation via

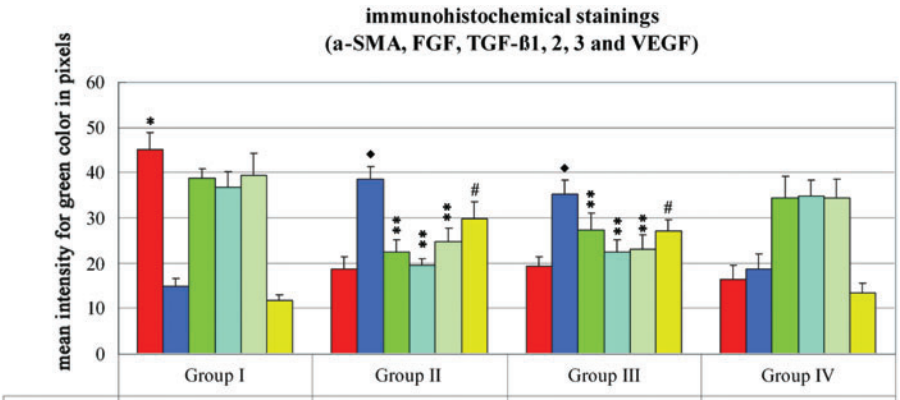

	Group I	Group II	Group III	Group IV
a-SMA	45.12	18.59	19.27	16.33
FGF	14.81	38.51	35.28	18.71
TGF-ß 1	38.84	22.37	27.18	34.41
TGF-ß 2	36.71	19.49	22.45	34.83
TGF-ß 3	39.52	24.72	23.15	34.37
VEGF	11.81	29.73	27.13	13.53

Figure 5. The immunohistochemical staining graph for alpha smooth muscle actin (α-SMA); fibroblast growth factor (FGF); transforming growth factor (TGF)-β1, -β2, and -β3; and vascular endothelial growth factor (VEGF). The anti–α-SMA antibody levels in groups II, III, and IV were statistically lower than group I (*$p<0.05$). The anti-FGF levels in groups II and III were statistically higher when compared with groups I and IV ($^{\blacklozenge}p<0.05$). The anti–TGF-β subfamily antibody levels were statistically lower in groups II and III (**$p<0.05$). The VEGF levels were statistically higher in groups II and III when compared with groups I and IV ($^{\#}p<0.05$). To see this illustration in color, the reader is referred to the web version of this article at www.liebertpub.com/wound

capillaries control the process by paracrine and autocrine effects. In addition, they supply the cell source for necessary differentiation.[1] Cellular phenotypic changes within the wound environment play an essential role in response to injury.[17] One of the most investigated changes is the transformation of fibroblasts into myofibroblasts. The key feature of these activated fibroblasts or myofibroblasts is the expression of α-SMA.[21] The contraction of the wound leads to faster epithelization as the defect area is forced to be smaller by the myofibroblasts. However, the mobility of the surrounding tissue might be hindered because of the tension. Therefore, in clinical cases of wound healing, surgeons prefer any treatment modality to prevent contraction but they seek for faster epithelization.

MSCs can differentiate not only into mesenchymal lineage cells but also into various other cell lineages. It was reported that MSCs can differentiate into multiple skin cell types including keratinocytes and contribute to wound repair.[22] Several studies in recent years suggested that MSCs, progenitor cells such as endothelial progenitor cells, and fibrocytes might have been involved in the healing process, contributing to skin cells or releasing regulatory cytokines. Direct injection of BSCs or endothelial progenitor cells into injured tissues showed improved repair through mechanisms of differentiation and/or release of paracrine factors.[23] In the present study, the differentiation of the BSCs and ASCs to endothelial cells and keratinocytes would not only help in the neovascularization but also help in the epithelization of the wound resulting in a faster healing.

The paracrine effect of the MSCs in the wound was described to be the main enhancer especially with the capability to increase FGF and VEGF levels.[24,25] Akasaka *et al.*[11] have shown that bFGF inhibited the expression of α-SMA leading to reduction of wound contraction. Lamme *et al.*[26] have described that the inhibitory effect on wound contraction was positively correlated with the number of fibroblasts seeded. However, the FGF-applied models have exhibited less contraction than the fibroblast-only groups, indicating the control on the apoptosis of the myofibroblasts and the transformation of the fibroblasts into myofibroblasts.[11] In addition, TGF-β is known to induce α-SMA expression in fibroblasts both *in vitro* and *in vivo*.[27] In this complex interaction of cells and growth hormones, FGF and TGF-β have an antagonist action. We have indicated low levels of α-SMA in the BSC and ASC groups when compared with the control group, indicating the decreased contraction of the wound. The high levels of FGF in the MSC-applied groups and the low levels of TGF-β subfamily also supported the α-SMA suppression enhanced by the BSCs and ASCs. The skin graft group had low

levels of α-SMA; however, the FGF, TGF-β, and VEGF levels were not much different from the control group, indicating that the main suppression of the contraction was caused by the epithelization from the patchy skin grafts.

The skin-grafted defects in clinical cases result in scar formation. The absence of the hair follicles in the skin grafts culminates in hairless scar formation. However, skin grafting enables faster epithelization and closure of the defect.[28,29] In our experimental model, the scar was larger in the skin-grafted, BSC, and ASC groups. A slower epithelization in a larger scar area without any skin grafting would be expected but the BSCs and ASCs resulted in a faster healing due to the increased FGF and VEGF levels. As correlated with the previous published data,[16,30–33] BSCs and ASCs fastened the healing process, increased the vascularity, increased the epithelial length, and formed a better scar tissue by the paracrine effect.

The characterization of MSCs by CD markers has been the golden standard. The debate on various CD marker positivity among different cell populations has been going on.[34,35] Although the purity of stem cells was not clearly analyzed in this study, our previous flow cytometric data on cell surface markers of cultured murine adipose-derived cells showed that ASCs of passage 3 expressed CD 11−/31−/34+/44+/45−/45R+/49d−/49e+/54+/81+/90-2+/106+/161c−/184+/c-kit-/Sca-1+, indicating that this cell population might be relatively pure and be called ASCs.[19,20]

Angiogenesis is a critical step in wound healing process.[36] VEGF and FGF are potent angiogenic factors. FGF application to wound was shown to increase granulation, decrease contraction, and increase angiogenesis.[11] In addition, TGF-β and FGF were clarified to activate fibroblast and keratinocyte proliferation and migration, collagen synthesis, and induce angiogenesis.[37,38] Any pharmacological agent, including growth hormones or cytokines, has a degradation half-life in the organism and the effect might be limited. Cell therapy, including MSCs, mainly BSCs and ASCs, for wound healing would benefit more as MSCs were described to be capable of expanding in number while showing a stable phenotype, multipotent to differentiate into other specialized cells, and secrete or suppress the growth hormones and cytokines necessary in the environment.[23,39]

AUTHOR DISCLOSURE AND GHOSTWRITING

The authors declare no conflicts of interest. This article was not written by any writer other than the authors.

KEY FINDINGS

- MSCs decrease acute wound contraction by blocking myofibroblasts.
- MSCs increase epithelization rate by paracrine effect on growth hormones and cytokines.
- MSCs decrease scar formation by paracrine effect on growth hormones and cytokines.

ABOUT THE AUTHORS

Cagri A. Uysal is a plastic surgeon and currently associate professor at the Department of Plastic and Reconstructive Surgery, Baskent University Faculty of Medicine, Ankara, Turkey. He has a PhD degrees in Clinical Anatomy and in Tissue Engineering and Stem Cells. He worked in the Department of Plastic and Reconstructive Surgery, Nippon Medical School, Tokyo, Japan, between 2005 and 2009. He has 75 internationally published articles in SCI, more than 100 national and international presentations, and won five international awards. He has written four book chapters. **Hiroshi Mizuno** is a plastic surgeon and currently professor and the chief at the Department of Plastic and Reconstructive Surgery, Juntendo University, Tokyo, Japan. He is among the authors who first described and published adipose-derived stem cells with Dr. Patricia Zuk. He has been a pioneer on stem cell research in Japan. He has more than 100 articles published internationally, national and international presentations, and awards. He has written book chapters and has been in editorial boards of international journals.

Morikuni Tobita is an oral-maxillofacial surgeon, DDS and currently associate professor at the Department of Plastic and Reconstructive Surgery, Juntendo University, Tokyo, Japan. He is the first researcher to have described the periodontal regeneration by using adipose derived stem cells and was awarded by the American Academy of Periodontology with the R. Earl Robinson Periodontal Regeneration Award in 2008.

Hiko Hyakusoku is a plastic surgeon and currently professor and the chief at the Department of Plastic and Reconstructive Surgery, Nippon Medical School, Tokyo, Japan. He has been one of the pioneers of plastic surgery in Japan. He has been well known among the international plastic surgery society with the techniques described and published including; prefabricated flaps, super thin flaps, propeller flaps. He has more than 200 published international articles. He has edited books, written chapters. He has been in editorial boards of international journals.

REFERENCES

1. Williams IR and Kupper TS: Immunity at the surface: homeostatic mechanisms of the skin immune system. Life Sci 1996; **58:** 1485.
2. Desmouliere A and Gabbiani G: Modulation of fibroblastic cytoskeletal features during pathological situations: the role of extracellular matrix and cytokines. Cell Motil Cytoskeleton 1994; **29:** 195.
3. Gabbiani G, Ryan GB, and Majne G: Presence of modified fibroblasts in granulation tissue and their possible role in wound contraction. Experientia 1971; **27:** 549.
4. Desmouliere A and Gabbiani G: The role of myofibroblast in wound healing and fibrocontractive diseases. In: *The Molecular and Cellular Biology of Wound Repair,* 2nd edition, edited by Clark RAF. New York, Plenum, 1996, pp. 321–323.
5. Desmouliere A, Chaponnier C, and Gabbiani G: Tissue repair, contraction, and the myofibroblast. Wound Repair Regen 2005; **13:** 7.
6. Gabbiani G: The myofibroblast in wound healing and fibrocontractive diseases. J Pathol 2003; **200:** 500.
7. Hinz B and Gabbiani G: Mechanisms of force generation and transmission by myofibroblasts. Curr Opin Biotechnol 2003; **14:** 538.
8. Arora PD and McCulloch CA: Dependence of collagen remodeling on alpha-smooth muscle actin expression by fibroblasts. J Cell Physiol 1994; **159:** 161.
9. Hinz B, Celetta G, Tomasek JJ, Gabbiani G, and Chaponnier C: Alpha-smooth muscle actin expression upregulates fibroblast contractile activity. Mol Biol Cell 2001; **12:** 2730.
10. Hinz B, Mastrangelo D, Iselin CE, Chaponnier C, and Gabbiani G: Mechanical tension controls granulation tissue contractile activity and myofibroblast differentiation. Am J Pathol 2001; **159:** 1009.
11. Akasaka Y, Ono I, Tominaga A, *et al.*: Basic fibroblast growth factor in an artificial dermis promotes apoptosis and inhibits expression of alpha-smooth muscle actin, leading to reduction of wound contraction. Wound Repair Regen 2007; **15:** 378.
12. Sporn MB and Roberts AB: A major advance in the use of growth factors to enhance wound healing. J Clin Invest 1993; **92:** 2565.
13. Gurtner GC, Callaghan MJ, and Longaker MT: Progress and potential for regenerative medicine. Annu Rev Med 2007; **58:** 299.
14. Rafii S and Lyden D: Therapeutic stem and progenitor cell transplantation for organ vascularization and regeneration. Nat Med 2003; **9:** 702.
15. Planat-Benard V, Silvestre JS, Cousin B, *et al.*: Plasticity of human adipose lineage cells toward endothelial cells: physiological and therapeutic perspectives. Circulation 2004; **109:** 656.
16. Fu X and Li H: Mesenchymal stem cells (MSCs) and skin wound repair and regeneration: possibilities and questions. Cell Tissue Res 2009; **335:** 317.
17. Goldberg MT, Han YP, Yan C, Shaw MC, and Garner WL: TNF-alpha suppresses alpha-smooth muscle actin expression in human dermal fibroblasts: an implication for abnormal wound healing. J Invest Dermatol 2007; **127:** 2645.
18. Spyrou GE and Naylor IL: The effect of basic fibroblast growth factor on scarring. Br J Plast Surg 2002; **55:** 275.
19. Ogawa R, Mizuno H, Watanabe A, Migita M, Shimada T, and Hyakusoku H: Osteogenic and chondrogenic differentiation by adipose-derived stem cells harvested from GFP transgenic mice. Biochem Biophys Res Commun 2004; **313:** 871.
20. Lu F, Mizuno H, Uysal CA, Cai X, Ogawa R, and Hyakusoku H: Improved viability of random pattern skin flaps through the use of adipose-derived stem cells. Plast Reconstr Surg 2008; **121:** 50.
21. Darby I, Skalli O, and Gabbiani G: Alpha-smooth muscle actin is transiently expressed by myofibroblasts during experimental wound healing. Lab Invest 1990; **63:** 21.
22. Sasaki M, Abe R, Fujita Y, Ando S, Inokuma D, and Shimizu H: Mesenchymal stem cells are recruited into wounded skin and contribute to wound repair by transdifferentiation into multiple skin cell type. J Immunol 2008; **180:** 2581.
23. Wu Y, Wang J, Scott PG, and Tredget EE: Bone marrow-derived stem cells in wound healing: a review. Wound Repair Regen 2007; **15 Suppl 1:** S18.
24. Hansen SL, Young DM, and Boudreau NJ: HoxD3 expression and collagen synthesis in diabetic fibroblasts. Wound Repair Regen 2003; **11:** 474.
25. Han SK, Yoon TH, Lee DG, Lee MA, and Kim WK: Potential of human bone marrow stromal cells to accelerate wound healing *in vitro*. Ann Plast Surg 2005; **55:** 414.
26. Lamme EN, Van Leeuwen RT, Brandsma K, Van Marle J, and Middelkoop E: Higher numbers of autologous fibroblasts in an artificial dermal substitute improve tissue regeneration and modulate scar tissue formation. J Pathol 2000; **190:** 595.
27. Desmouliere A, Geinoz A, Gabbiani F, and Gabbiani G: Transforming growth factor-beta 1 induces alpha-smooth muscle actin expression in granulation tissue myofibroblasts and in quiescent and growing cultured fibroblasts. J Cell Biol 1993; **122:** 103.
28. Ramasastry SS: Acute wounds. Clin Plast Surg 2005; **32:** 195.
29. Moreira ME and Markovchick VJ: Wound management. Emerg Med Clin North Am 2007; **25:** 873.
30. Yoshikawa T, Mitsuno H, Nonaka I, *et al.*: Wound therapy by marrow mesenchymal cell transplantation. Plast Reconstr Surg 2008; **121:** 860.
31. Stoff A, Rivera AA, Sanjib Banerjee N, *et al.*: Promotion of incisional wound repair by human mesenchymal stem cell transplantation. Exp Dermatol 2009; **18:** 362.
32. Kwon DS, Gao X, Liu YB, *et al.*: Treatment with bone marrow-derived stromal cells accelerates wound healing in diabetic rats. Int Wound J 2008; **5:** 453.
33. Nambu M, Ishihara M, Nakamura S, *et al.*: Enhanced healing of mitomycin C-treated wounds in rats using inbred adipose tissue-derived stromal cells within an atelocollagen matrix. Wound Repair Regen 2007; **15:** 505.
34. Tomiyama K, Murase N, Stolz DB, *et al.*: Characterization of transplanted green fluorescent protein+ bone marrow cells into adipose tissue. Stem Cells 2008; **26:** 330.
35. Niemeyer P, Kornacker M, Mehlhorn A, *et al.*: Comparison of immunological properties of bone marrow stromal cells and adipose tissue-derived stem cells before and after osteogenic differentiation *in vitro*. Tissue Eng 2007; **13:** 111.
36. Seifter E, Rettura G, Padawer J, Stratford F, Kambosos D, and Levenson SM: Impaired wound healing in streptozotocin diabetes. Prevention by supplemental vitamin A. Ann Surg 1981; **194:** 42.
37. Slavin J: The role of cytokines in wound healing. J Pathol 1996; **178:** 5.
38. Greenhalgh DG: The role of growth factors in wound healing. J Trauma 1996; **41:** 159.
39. McFarlin K, Gao X, Liu YB, *et al.*: Bone marrow-derived mesenchymal stromal cells accelerate wound healing in the rat. Wound Repair Regen 2006; **14:** 471.

Abbreviations and Acronyms

ASCs = adipose-derived stem cells
BSCs = bone-marrow-derived stem cells
FBS = fetal bovine serum
FGF = fibroblast growth factor
FITC = fluorescein-isothiocyanate
HE = hematoxylin and eosin
MSCs = mesenchymal stem cells
PBS = phosphate-buffered saline
TGF-β = transforming growth factor beta
VEGF = vascular endothelial growth factor
α-SMA = alpha smooth muscle actin